AD-A154 056 INJECTION ATOMIZATION IGNITION AND COMBUSTION OF LIQUID FUELS IN HIGH-SPE..(U) VIRGINIA POLYTECHNIC INST AND STATE UNIV BLACKSBURG DEPT OF A.. J A SCHETZ JAN 84 1/1

UNCLASSIFIED VPI-AERO-136 AFOSR-TR-85-0382 AFOSR-82-0159 F/G 21/4 NL

END
FILMED
DTIC

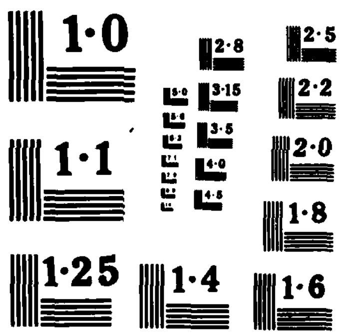
1·0
2·8
2·5
3·15
2·2
3·5
2·0
1·1
4·0
4·5
1·8
1·25
1·4
1·6

COLLEGE OF ENGINEERING

AFOSR Annual Scientific Report — Jan. 1984
Grant AFOSR 82-0159 — VPI-AERO-136

INJECTION, ATOMIZATION, IGNITION AND COMBUSTION OF LIQUID FUELS IN HIGH-SPEED AIR STREAMS

Joseph A. Schetz

Aerospace and Ocean Engineering Department

VIRGINIA POLYTECHNIC INSTITUTE AND STATE UNIVERSITY

BLACKSBURG, VIRGINIA

AFOSR Annual Scientific Report
Grant AFOSR 82-0159

Jan. 1984
VPI-AERO-136

INJECTION, ATOMIZATION, IGNITION AND COMBUSTION OF LIQUID FUELS IN HIGH-SPEED AIR STREAMS

Joseph A. Schetz

Aerospace and Ocean Engineering Department

UNCLASSIFIED

SECURITY CLASSIFICATION OF THIS PAGE (When Data Entered)

REPORT DOCUMENTATION PAGE

READ INSTRUCTIONS BEFORE COMPLETING FORM

1. REPORT NUMBER AFOSR-TR- 85-0382	2. GOVT ACCESSION NO. AD-A154056
3. RECIPIENT'S CATALOG NUMBER	
4. TITLE (and Subtitle) Injection, Atomization, Ignition and Combustion of Liquid Fuels in High-Speed Air Streams	5. TYPE OF REPORT & PERIOD COVERED Annual 1 Dec. 1982 - 30 Nov. 1983
	6. PERFORMING ORG. REPORT NUMBER VPI-Aero-136
7. AUTHOR(s) J. A. Schetz	8. CONTRACT OR GRANT NUMBER(s) AFOSR-82-~~1059~~ 0159
9. PERFORMING ORGANIZATION NAME AND ADDRESS Virginia Polytechnic Institute and State Univ. Aerospace and Ocean Engineering Department Blacksburg, VA 24061	10. PROGRAM ELEMENT, PROJECT, TASK AREA & WORK UNIT NUMBERS 61102F 2308/A2
11. CONTROLLING OFFICE NAME AND ADDRESS Air Force Office of Scientific Research/NA Bolling Air Force Base, DC 20332	12. REPORT DATE Jan. 1984
	13. NUMBER OF PAGES
14. MONITORING AGENCY NAME & ADDRESS (if different from Controlling Office)	15. SECURITY CLASS. (of this report) Unclassified
	15a. DECLASSIFICATION/DOWNGRADING SCHEDULE

16. DISTRIBUTION STATEMENT (of this Report)

Approved for Public Release; distribution unlimited.

17. DISTRIBUTION STATEMENT (of the abstract entered in Block 20, if different from Report)

18. SUPPLEMENTARY NOTES

Tsubo

19. KEY WORDS (Continue on reverse side if necessary and identify by block number)

Ramjets
Liquid Jets
Combustors
Slurries

20. ABSTRACT (Continue on reverse side if necessary and identify by block number)

Experimental and numerical studies of liquid and slurry jet penetration, break-up and atomization were performed. The measurements were done mainly at Mach 3.0 with P_0 = 4 atm. and T_0 = 300°K. Brief summaries of recent progress on various tasks are given.

DD FORM 1 JAN 73 1473 EDITION OF 1 NOV 65 IS OBSOLETE

UNCLASSIFIED

SECURITY CLASSIFICATION OF THIS PAGE (When Data Entered)

Abstract

Experimental and numerical studies of liquid and slurry jet penetration, break-up and atomization were performed. The measurements were done mainly at Mach 3.0 with P_0 = 4 atm. and T_0 = 300°k. Brief summaries of recent progress on various tasks are given.

Research Objectives

Activity in the ramjet/scramjet field continues to grow due to the potential performance benefits for missile, projectile, aircraft and orbiter propulsion. The complex physical and chemical processes resulting from injection of liquid and/or liquid-slurry fuel jets into high speed airstreams find direct application there and in several other propulsion-related systems. For supersonic airstreams, these include thrust vector control and external burning in the wake region of projectiles, as well as scramjet engines. For subsonic airstreams, the other applications include "dump" combustors on devices such as integral rocket ramjets, afterburners and dumping of cooling water out the end of turbine blades, in addition to subsonic ramjet devices.

The important phenomena in all of these applications include physical processes associated with gross penetration; jet fracture, breakup and atomization; phase separation and, in some, chemical processes associated with ignition and combustion. Studies at Virginia Tech during the subject time period concentrated on various aspects of the complex physical processes involved.

Distribution of Injectant in the Spray Plume

The distribution of the mass of injectant across any transverse plane in the spray plume is important for ignition, efficient combustion and smoke and pollutant production considerations. For liquid-slurry injectants the spatial separation of the phases due to the processes of penetration and jet breakup is of interest. This is especially true, since some proposed systems would rely upon combustion of the liquid phase to ignite the solid phase. Perhaps surprisingly, there is very little prior work in the literature even for the simpler all-liquid injectant use. Our objective this year was to conduct a thorough experimental study under a set of representative conditions.

Effects of Mass Transfer on Jet Breakup

Almost all previous, basic studies of the complex processes of liquid jet breakup have neglected the effects of mass transfer. This is the case for both analytical and experimental studies of a fundamental nature. For the case of fuel jets, this is a serious limitation, since large mass transfer rates are to be expected. Our objective was to undertake a basic, combined analytical and experimental study of the idealized case of a laminar jet in a co-flowing air stream including the effects of significant rates of heat and mass transfer during the breakup process. This would be a first step towards treating the very complex situation encountered in a combustion chamber.

Status of the Research

Distribution of Injectant in the Spray Plume

Liquid and slurry jets were injected through a circular orifice transversely to a M=3.0 airflow. Mass samples of both jets were taken across the plume 30 injector diameters downstream. A mass flow distribution was determined for each case. Pitot and static pressure surveys were taken across the liquid jet, and these data allowed the calculation of a Mach number distribution in the liquid jet plume.

The results of the sampling for the all-liquid jet case are presented in Fig. 1 in terms of mass flow per unit area. This is one half of the x/d=30 plane of the jet. Figure 1a shows the shape of the distribution and Fig. 1b shows the numerical values.

The actual cross-stream penetration of the jet at this station and how it compares with penetration estimates as compiled from photographic techniques is the first result. It can be seen that trace amounts of samples were collected at 19 injector diameters high, but, neglecting these as negligible, z/d=18 could be called the penetration. Samples at z/d=18 are roughly 4.0% of the maximum sample size on the centerline y/d=0. Yates and Rice obtained an empirical equation for water penetration from a circular injector into a cross flow that predicts h/d=14.6 or 19% below the actual penetration of h/d=18. Fig. 1b also allows the width of the jet at x/d=30 to be determined. The data shows that by y/d=-10, $\dot{m}/A$ is generally under 6% of the centerline value at that value of z/d. Joshi and Schetz give an expression for jet width which yields w/d=15.8 or 21% below the present value of w/d=20. Thus photographic techniques seriously underestimate the dimensions of the liquid jet plume.

An integration of the mass flow across the x/d=30 plane from the sampling data resulted in a mass flow of 67 gm/sec or 75% of the mass flow through the injector. Based on photographs showing a sizable liquid surface layer at test conditions similar to those here, it is believed that a substantial portion of the injected mass flow not accounted for in the samples is carried in the liquid layer. Conservative estimations show that this is quite probable.

Fig. 2a shows data taken in the -y/d half plane for the nominally 30% loaded slurry jet. Both the average local particle loading of the samples and the total mass flow per unit area are shown. As expected, the loading increases smoothly in the +z/d direction from z/d=2 to z/d=10 then jumps sharply at z/d=12 to almost triple the value at z/d=2. This increased loading is due to the heavier particles following paths with greater radii of curvature due to their greater inertia and thus separating from the liquid plume consistent with the visual observations of Less and Schetz. Perhaps unexpectedly the same phase separation was noticed side-to-side in the -y/d direction at both z/d=2 and z/d=10. The same trend was evident in the +y/d direction at the same z/d values as is shown in Fig. 2b.

More detailed results are given in AIAA Paper No. 84-0041. The main conclusions are summarized here.

1. The actual penetration and width of the all-liquid jet at x/d=30 were approximately 20% above that determined from photographic techniques.

2. Mass flow data indicate that the slurry and liquid jets are both asymmetrical about the centerline axis. This along with additional sampling and pressure data indicate that there is a possibility of low frequency oscillations of the jet in the side-to-side direction.

3. The cross section of the jet plume has at least two clearly defined regions. There is a core region which has high subsonic velocity and a relatively constant mass flow in the side-to-side direction at a given vertical location along with low total pressure. For the liquid jet at 30 injector diameters downstream the core occupies one-third

of the plume area but carries two-thirds of the plume mass flow. Surrounding the core region is the peripheral mixing region characterized by supersonic velocities, increasing total pressures and decreasing mass flows. The region is unsteady in its location.

4. Substantial phase separation in the slurry jet plume was found. The local loadings were only one-third of the injected value in the center of the jet and increased significantly as the boundary of the plume is approached from any direction.

Effects of Mass Transfer on Jet Breakup

One aspect of the jet breakup problem that has received little prior study is the effect of rapid surface mass transfer on the breakup process. This is particularly important in propulsion applications where a cool fuel jet is often injected into hot gaseous surroundings. This report will present some results of a coordinated computational and experimental study.

The computational work uses a substantially extended and generalized version of the Marker-and-Cell (MAC) code originally developed at Los Alamos. This method has proven useful for problems involving free surface phenomena. Our efforts have focussed on generalizing the boundary conditions to permit computations for a flowing jet and, most importantly, extensions to treat surface mass transfer and diffusion of the injectant vapor into the surroundings air stream. A few results are shown in the attached figures. Two observations can be made. First, surface mass transfer is generally stabilizing at conditions near the disturbance wavelength for maximum growth. Second, non-linear effects are important in determining the disturbance wavelength with the greatest growth rate. For very small amplitudes, the numerical results agree with the classical, linear Rayleigh analysis. As the amplitude grows, however, other wavelengths show greater growth rates.

The experiments are conducted using heated water and Methanol as the injectants. The growth of surface disturbances until jet breakup and the resulting drop sizes are measured optically. Results have been presented over a range of the pertinent parameters and compared to the numerical predictions.

Fig. 3 shows the instantaneous jet shape from the numerical solution plotted by computer. At jet breakup, when the nondimensional time is 9.03, the jet shape from the numerical solution is very similar to that at breakup from the experiments. The shapes of the Methanol jet surface, both from numerical prediction and from experiment are presented in Fig. 4. Basically, they are identical, but the jet shape from experiment appears to be thinner than the shape predicted by numerical result. In Fig. 5 is shown the relation of the nondimensional perturbation amplitude against the nondimensional time. It is obvious that before the breakup of the Methanol jet, the nondimensional perturbation amplitude of the crest first decreased. The experimental results and numerical results both showed this phenomena, but the experimental effect was less than found by numerical solutions.

More detailed results are given in AIAA Paper No. 83-1400. The principal results are listed below:

1. In the regime of low speeds of the coaxial gas stream, a small axisymmetric perturbation which is spatially sinusoidal along the length of the column grows, and this leads to breakup. The numerical solution

can predict the jet shape and breakup time in the lower air velocity regime.

2. The numerical solution and the experimental results both indicate that the wave number of the maximum instability is about 6.9. When the instantaneous perturbation amplitude of the jet is very small, the wave number of maximum instability is close to 4.51 which was predicted by Rayleigh's theory.

3. The experimental results showed that the perturbation amplitude of the crest and the perturbation amplitude of the trough were different. The growth of the amplitude of the trough is faster than the growth of the crest amplitude. This is identical with the prediction of the numerical solution.

4. For small heat and mass transfer rates, it was found that the interface evaporation and the variation of the interface temperature had a destabilizing effect when the wave number is large or small.

Professional Personnel

Dr. Joseph A. Schetz

Interactions

Various groups in government, universities and industry here and abroad continue to use our results that are published in the open literature for design and to support further research. Recently, we have also been contacted directly by engineers from the Atlantic Research Corp., Northrup, Aerojet General, Rocketdyne, NASA Langley Research Center and Applied Physics Lab., Johns Hopkins University.

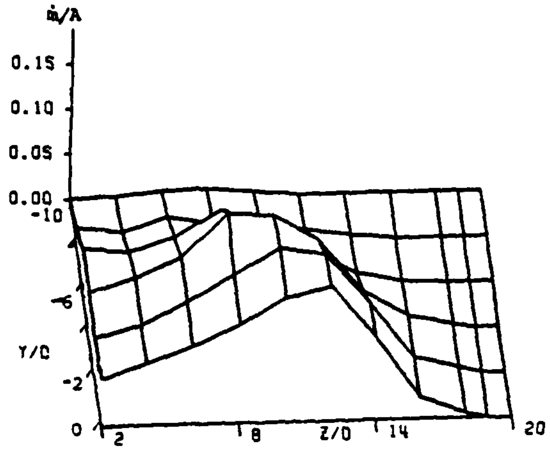

a. Graphical Distribution

Z/D \ Y/D	0	-2	-4	-6	-8	-10
20						
19	0.0009	0.0005				
18	0.0058	0.0060	0.0035			
16	0.0241	0.0182	0.0141	0.0024		
14	0.0911	0.0779	0.0413	0.0124	0.0048	
12	0.1475	0.1328	0.0989	0.0358	0.0116	0.0005
10	0.1354	0.1403	0.1265	0.0617	0.0186	0.0045
8	0.1080	0.1127	0.1031	0.0841	0.0182	0.0079
6	0.0848	0.0834	0.0831	0.0558	0.0285	0.0069
4	0.0683	0.0603	0.0622	0.0406	0.0138	0.0023
2	0.0523	0.0468	0.0474	0.0456	0.0186	0.0006

b. Numerical Values

Fig. 1 Mass flow per unit area ± 0.0002 [gm /s-mm^2] in the x/d=30 plane for the liquid jet.

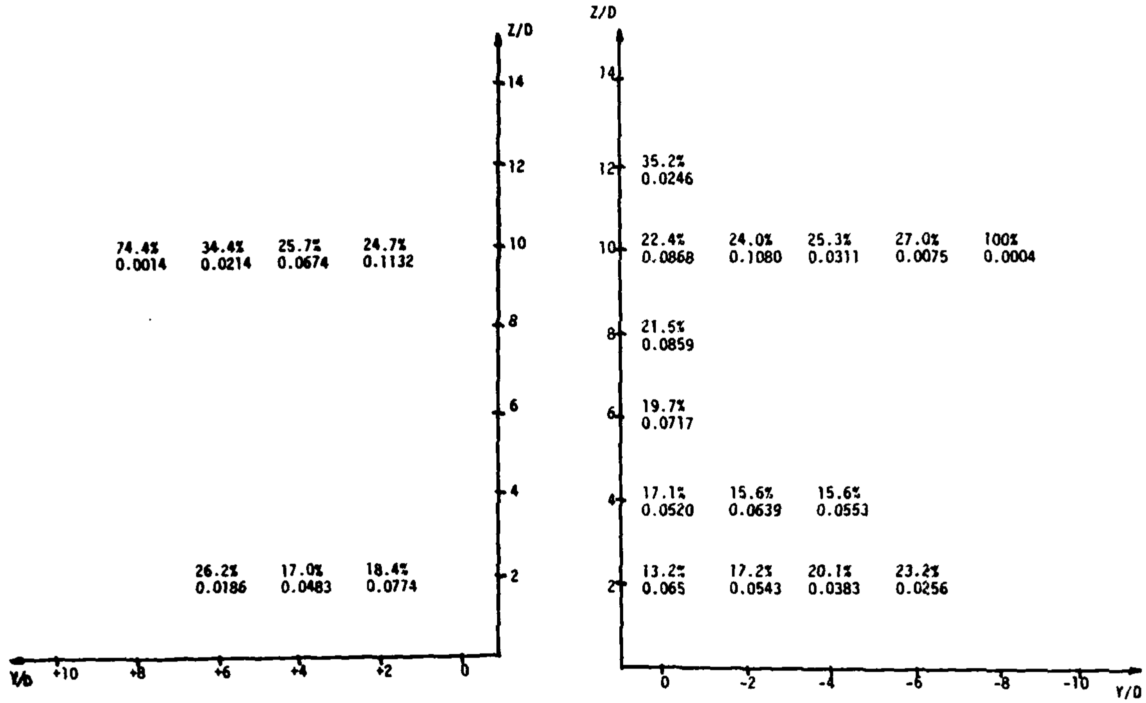

b. +y/d half plane.

a. -y/d half plane.

Fig. 2 $\dot{m}/A \pm 0.0003$ [$gm/s\text{-}mm^2$] in the x/d=30 plane for the slurry jet, also the local loading of the slurry.

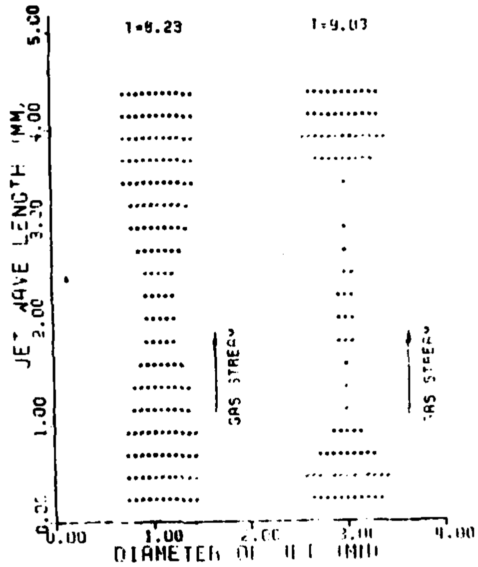

Fig. 3 - Fluid Configuration Calculated for Jet; V_a=2.0 (m/s) WN=5.43 ,T_F=302 °K ,T_a=299 °K

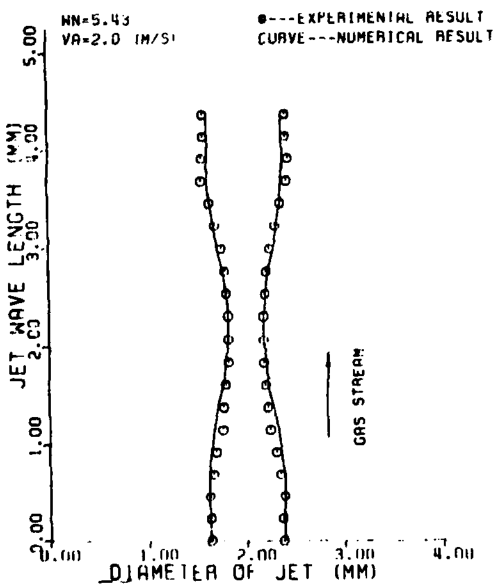

Fig. 4 - Numerical Prediction of Surface Shape Compared with Surface Shape from Experiment at T=8.234; T_F=302 °K , T_a=299 °K

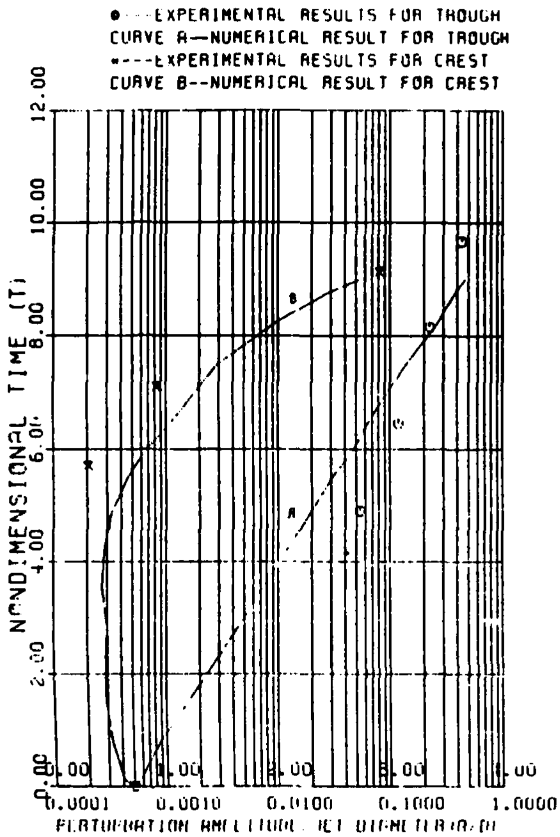

Fig. 5 - Perturbation Amplitude Plotted against Nondimensional Time ; V_a=2.0 (m/s), WN=5.43 , T_F=302 °K ,T_a=299 °K

END

FILMED

6-85

DTIC